Original Article

A Novel Application of Zinc Oxide Nanoparticles for Inhibition of *Molluscum contagiosum* Virus Infection

Almansorri, A. K[1], Al-Shirifi, H. M. H[2], Al-Musawi, S[3] *, Ahmed, B. B[1]

1. Faculty of Biotechnology, Al-Qasim Green University, Babylon, Iraq
2. Environmental Health Department, Environmental Sciences College, Al-Qasim Green University, Babylon Province, Iraq
3. College of Food Sciences, Al-Qasim Green University, Babylon Province, Iraq

Abstract

Molluscum contagiosum virus (MCV) is an infection caused by the *molluscum contagiosum virus*. Antiviral medications used to treat MCV infections have several problems, including drug-resistant and toxicity. As a result, improving safe, innovative, and effective antiviral drugs is critical. Therefore the current study aimed to investigate ZnO-NPs effects on *M. contagisum* infection and *molluscum contagiosum virus* replication, among the main exciting viruses that menace human health. The antiviral activity of zinc oxide nanoparticles (ZnO-NPs) against MCV infection was investigated in this work. FESEM and TEM electron microscopy were used to examine the nanoparticles. The cytotoxicity of the nanoparticles was assessed using the MTT assay, and anti-influenza effects were detected using RT-PCR and TCID50. An indirect immunofluorescence experiment was used to investigate the inhibitory effect of nanoparticles on viral antigen expression. In all tests, acyclovir was employed as a control. Compared to virus control, post-exposure of MCV with ZnO nanoparticles at the highest dose but is not toxic (100 g/mL) resulted in 0.2, 0.9, 1.9, and 2.8 log10 TCID50 reductions in infectious diseases virus titer (P=0.0001). This ZnO-nanoparticles level was accompanied by an inhibition percentage (17.8%, 27.3%, 53.3%, 62.5 %, and 75.9%), respectively, measured based on viral load compared with the virus control. Compared to the positive control, fluorescence emission intensity in virally infected cells that administrated ZnO nanoparticles was statically decreased. Our findings demonstrated that ZnO-NPs have antiviral effects against the MCV. This property indicates that ZnO-NP has a high potential for usage in topical formulations to treat facial and labial lesions.

Keywords: Molluscum contagiosum virus, Zinc oxide nanoparticles, Antiviral activity

1. Introduction

MCV is a skin condition caused by the MCV, a huge brick-shaped poxvirus with double-stranded DNA that replicates in the cytoplasm of cells. It has several genetic features in common with other poxviruses (1, 2). The usual lesion is dome-shaped, spherical, and pinkish-purple in colour, and the skin lesion could stay for months to years before cure (3). Furthermore, they only affect children and adults, especially immunocompromised people, and they only affect the skin. Skin, sexual, and autoinoculation contact are done by scratching, and the MCV is transferred by indirect route by contaminated fomites (4, 5). The MCV virus has four subtypes, the most common of which is MCV-1 (98 % of cases) in children, whereas MCV-2 is mainly responsible for skin lesions in HIV patients. In Asia and Australia, MCV-3 and MCV-4 are available. Currently, MCV cultures are not possible (6, 7). Physical therapy or chemical agents are currently used to treat MCV; although they are not always safe or effective, they frequently fail the treatment the lesions, then leading to generating the scar (8).

Furthermore, Cidofovir is a wide-spectrum antiviral used as an intravenous or topical medicine for MCV in patients with low immune, but it has adverse effects such as erosion, inflammation, and discomfort if applied topically and possible nephrotoxicity when used systemically (3). No single antiviral medicine is available for the treatment of MCV at this time (9). The virus's incapacity to proliferate in culture has delayed the development of safe antiviral drugs (10). NPs offer unique physical properties and have been developed to treat infectious diseases (11-13). These are primarily attributed to the particle size, which influences bioavailability and circulation time, and the wide area-by-volume ratio (increased solubility compared to larger particles). Such properties make ideal nanoparticulate candidates for investigating and enhancing therapeutic impacts (14-19). Nanotechnology-based antiviral treatments and metal nanoparticles have been appealing and effective against various viruses in recent years (20). ZnO-NPs, a bio-safe material with optical, chemical sensing, electric conductivity, catalytic, and photochemical properties, have been found to have antimicrobial activity against a variety of human pathogens due to increased specific surface area as a result of reduced particle size leading to increased particle surface reactivity (21-23). However, most studies studied inhibition activity on microbial infections, with only a few examining the interaction of ZnO-NPs with viruses. In this regard, the current study aimed to investigate ZnO-NP's effects on *M. contagisum* infection and replication, among the main exciting viruses that menace human health.

2. Materials and Methods

2.1. The Used Materials

Merck Company provided powdered ZnO-NPs for this study (Germany; Catalogue Number: 108846). To make varied quantities of nanoparticles, they were added to Dulbecco's Modified Eagle (Shangdong, Yantai, China) and submitted to sonicated to remove the accumulative. Acyclovir (Sigma, China) was diluted in DMEM and used at various concentrations as a standard treatment against MCV.

2.2. Characterization of Nanoparticles

High-resolution transmission electron microscopy and Field emission scanning electron microscopy was used to obtain morphological, dimensional and size data about NPs.

2.3. Culture of the Virus and Cells

The BHK-21 cells were donated from the National Cell Bank of Iran's Pasteur Institute, Tehran. DMEM is used for culture of the BHK-21 cells with 10% fetal bovine serum (Gibco, USA), sodium pyruvate 1 mM (Merck, Germany), streptomycin 100 IU/mL, and penicillin 100 g/mL (Merck, Germany), L-glutamine 2 mM (Merck, Germany). The cells were cultivated at 37°C in the incubator with 5% CO_2. The MC viral stock was donated by Tarbiat Modares University's Virology Department (Tehran, Iran), reproduced in BHK-21 cells, titrated using the Reed and Muench procedure, and kept in the vials at (70) °C.

2.4. Cytotoxicity Assay

The impact of ZnO-nanoparticles on the BHK-21 cells was examined using the methyl thiazolyl tetrazolium method. A day of incubation at 37°C was spent cultivating BHK-21 cells at a density of 1 105 cells/mL on a microtiter plate with a flat bottom (Nalge Nunc, Naperville, IL) and incubating for one day. In this experiment, multiple concentrations of ZnO-NPs (20 to 140 g/mL) were applied to the plate in triplicate. Incubation for two days at 37°C was followed by adding 10 ml (5 mg/mL) MTT reagent (Roche, Germany) into each well and incubating in an atmosphere without light for 180 minutes at 37°C before the results were analyzed. Remove the MTT solution and replace it with 50 mL of ordinary dimethyl sulfoxide (Sigma, USA), then shake it at 25 degrees Celsius for ten minutes. In the end, the plate in a microplate reader (Synergy, USA)was read at (550) nm, and the cell viability rate was determined for each level compared to the control cells on the plate.

2.5. Determination of Antiviral Activity

Confluent monolayers of BHK-21 cells were treated for 60 minutes at (37°C)with CO_2 5% in the microtiter plate (96 wells) with 100 L of 100 TCID50/mL MCV. Monolayers were washed three times with PBS after the viral inoculation removed any viruses. The cells were grown for two days at 37°C in CO_2 5% atmosphere with (100)L of different noncytotoxic dosages of ZnO-NPs. There was also cell control and viral control in this experiment. This approach was also used to test acyclovir. Following incubation, the cells were frozen and thawed again to allow the virus particles to be released from the cells. The good lysates were collected and employed in TCID50 and quantitative RT-PCR experiments at the end of the process.

2.6. Quantitative Real-Time PCR Assay

According to the manufacturer's instructions, the Genomic DNA Extraction Mini kit (Qiagen, UK) was used to extract MC viral DNA from the collected lysate. In a Real-Time quantitative PCR, a 65-bp fragment of the L1 region was amplified using the primers 5′-GAGAACTGCAATGTTTCAGGACC3-3′ and 5′-TGTATAGTTGTTTGCAGCTCTGTGC3-3′ (Detection and genotyping of human MCV by real-time PCR assay). For RT-PCR, the reactions and temperature were the same as in the prior work [28]. The RT-PCR was carried out using Rotor-Gene Q equipment (Qiagen, UK). As a template, a recombinant plasmid containing a 65-bp DNA fragment from the MCV's L1 gene was constructed using a recombinant plasmid. Amplification and cloning of the section into the PGH vector were carried out before the section was given as a lyophilized powder. General Biotech was in charge of creating recombinant plasmids and cloning these plasmids (Shanghai, China). When four grammes of the template were combined with forty litres of dilution buffer, the result was a stock solution with a concentration of one hundred nanograms per millilitre (ng/mL) for the standard solutions. Following the acquisition of the DNA concentration by NanoDrop, the number of DNA copies in the standard stock was calculated using software developed by the URI Genomics & Sequencing Center (Fisher, USA). The stock solution was tenfold serially diluted to produce standard curves and utilized as a template to create the standard curves. By comparing the unknown samples to the standards, it was possible to determine the amount of MC virus copies present.

2.7. Indirect Immunofluorescence Assay (IFA)

BHK-21 cells were seeded and grown in the wells of a 24-well tissue culture plate with sterile glass coverslips (Sigma-Aldrich, USA) using sterile glass coverslips (Qiagen, UK). In a humidified environment at 37 degrees Celsius with carbon dioxide5%, cells were allowed to attain 80 % confluence before the media was removed from the wells, and 200 L of 100 TCID50/mL MCV was suspended for 1 hour in the absence of a medium. Incubation at 37°C with the greatest noncytotoxic dose of ZnO-NPs was performed after the viral inoculum was removed. Additionally, this experiment included a cell control (treated uninfected cells) and a viral control (untreated infected cells). The cells were fixed with cold acetone for 15 minutes after 14 hours of incubation, then treated with MCV, a particular human antibody, for 45 minutes at room temperature. After three washes with PBS, the cells were treated for 40 minutes at room temperature with goat anti-human IgG conjugated with fluorescein isothiocyanate (FITC) (Sigma-Aldrich, USA). The labelled cells were rinsed three times in PBS before being examined with an Olympus fluorescence microscope (Tokyo, Japan).

2.8. Statistical Analysis

The mean of the three samples, as well as the standard deviation, are represented by the data. The comparisons were made using one-way ANOVA, followed by Tukey's multiple tests, performed using GraphPad Prism at a p-value of less than 0.05.

3. Results

3.1. Characterization

DLS-determined Al$_2$O$_3$-NPs were found at 120.8±21.7 nm with 0.126±0.05 mV polydispersity index (PDI) (Figure 1A). As shown in figure 1B, the crystal structure of the Al$_2$O$_3$-NPs was studied with XRD. All nine diffraction peaks' position and relative strength corresponded well to the Normal Al$_2$O$_3$-NPs XRD sequence, comparable with the spectra previously mentioned (Figure 1B) (20, 23). Morphology of Al$_2$O$_3$-NPs and their size Characterized by using FESEM and DLS techniques. FESEM images showed spherically distributed Al$_2$O$_3$-NPs with identical particle shape, size distribution, and 120 nm mean diameter (Figures 2A and 2B).
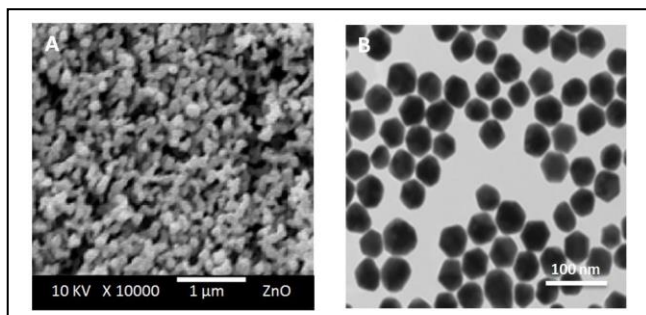

Figure 1. A) FESEM picture of ZnO-NPs (X10 kx); TEM image of ZnO-NPs (X10 kx). **B)** Particle size and shape distribution of ZnO-NPs were determined, and the results showed a spherical shape with a mean size (35) nm and a uniform shape and size distribution
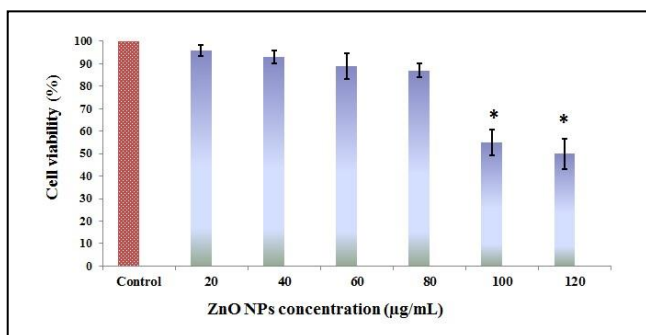

Figure 2. The MTT test was used to determine the cytotoxic impact of ZnO-NPs on the Vero cell line

3.2. MTT Results

The results demonstrate that increasing the ZnO-NPs level to 120 g/mL lowered cell viability to 60.03% compared to control cells (Figure 2). The MTT method was used to assess the cytotoxic effect of ZnO-NPs on BHK-21 cells infected with the MCV (Figure 2). That shows the viability of BHK-21 cells exposed to ZnO-NPs at 20, 40, 60, 80, 100, and 120 g/mL (P=0.0001). As the concentration of ZnO-NPs was increased to 120 g/mL, the cell viability dropped to 48.32% compared to control cells. Vertical lines represent three different experiments' mean values. Compared to control cells, cell viability dropped to 60.03%.

The curve demonstrates that when the quantity of ZnO-NPs was increased to 120 g/mL, the cell viability decreased to 60.03% compared to the control cells (Figure 1). The vertical lines reflect the mean results of three experiments; horizontal lines show the standard deviation.

3.3. Cytopathic Effects (CPE)

TCID50 assay was used to compare the viability of BHK-21 cells and the antiviral effect of ZnO -NPs on the MCVinfection titer. When MCV-infected BHK-21 cells were exposed to 20, 40, 80, and 100 g/mL ZNO-NPs, the infectious titer of the MCVwere reduced by 0.3, 1.1, 2.3, and 3.3 log10 TCID50, respectively, compared to virus control (Figure 3).

3.4. Evaluation of Antiviral Activity

ZnO-NPs have been shown to have cytotoxic effects on BHK-21 cells infected with MCV; this research indicated that infected MCV BHK-21 cells treated with 100 g/ml of ZnO-NPs had cytotoxic effects. The creation of syncytia and cell rounding are three separate cytopathic effects that occur in the organism's body. Vero cells infected with M. contagiosum treated with ZnO-NPs showed reduced cytotoxic effects. Notably, the TiO2-NP at the highest concentration tested (100 g/ml) was linked with a cytotoxic impact on the BHK-21 cells in the range of 10% to 15% cytotoxicity. Consequently, the morphology of cells in specific locations differs from the cell control, which is not connected to MCV-induced cytopathic effects, as was previously stated (Figure 4).
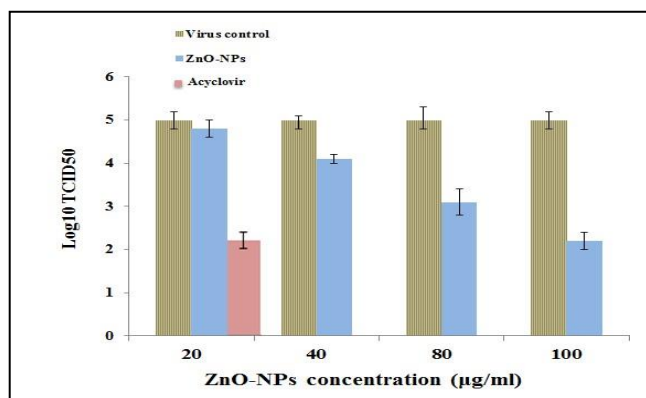
Figure 3. The antiviral effect of ZnO-NPs on the MCV infectious titer was determined using the TCID50 test and compared to that of acyclovir. As MCV-infected cells were exposed to 20, 40, 80, and 100 ng/mL ZnO-NPs, the infectious titer of MCV decreased by 0.2, 0.9, 1.9, and 2.8 log10 TCID50, respectively, when compared to viral control
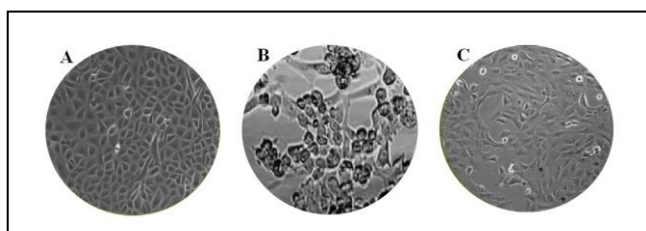

Figure 4. In the presence of ZnO-NPs, the inhibition of MCV-produced cytopathic effects on Vero cells was observed. (A) Cell control, (B) virus control, and (C) MCV-infected cells treated with 100 g/ml of ZnO-NPs were shown

As seen in figure 4, MCV induced diverse cytopathic effects, including cell rounding, refringence, and the development of syncytia, which were all observed. It was possible to minimize the cytotoxic effects of M. Contagiosum infection in Vero cells treated with ZnO-NPs. Notably, the ZnO-NP at the highest concentration tested (100 g/ml) was linked with a cytotoxic impact on the Vero cells, about 10% higher than the control. As a result, the morphology of the cells has been changed in specific locations as compared to the control cells, and this is not associated with the cytopathic effects of MCV.

3.5. RT PCR

5-RT-PCR was used to analyze the influence of ZnO-NPs on MCV load. The 127-bp fragment amplification from a US3 gene MCV region was done using SYBR Green Q-PCR to determine the effect of ZnO-NPs on MCV load. Following figure 5, the effect of ZnO-NPs on MCV load was assessed by real-time PCR. MCV-based estimates of the inhibition rates for ZnO-NPs at concentrations of 20, 40, 60, 80, and 100 g/mL revealed that they produced 24.9 %, 35.1 %, 47.2 %, 59.5 % and 66.6 % inhibition rates, respectively when used in conjunction with MCV-based estimates (Figure 5).

3.6. IFA Assay

To investigate the inhibitory effects of ZnO-NPs on the expression of antigens MC virus on the surface of BHK-21 cells, the researchers employed an IFA test, which revealed that the compounds were effective. In this investigation, we detected the effect of ZnO-NPs on the expression of MCV antigens on BHK-21 cells using an immunofluorescence assay (IFA). As a consequence of the findings, virus control, cell control, and MCV-infected cells were all treated with 100 g/mL ZnO-NPs in the presence of the virus. This work found that the fluorescence signal intensity of MCV-infected cells treated with ZnO-NPs was significantly decreased compared with virus control, suggesting that TiO2—NPs had a significant antiviral impact on MCV antigen expression when compared with virus control (Figure 6). Virus antigens were expressed in different cell compartments, as shown by the green dots in Figure 6C, stained with goat anti-human IgG combined with fluorescein Isothiocyanate to visualize viral antigen expression in each compartment (FITC).
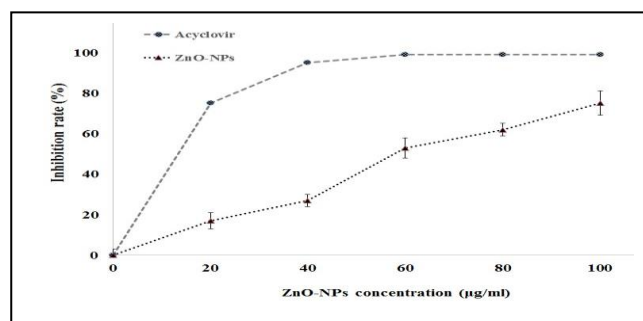

Figure 5. The effect of ZnO-NPs on the viral load of the MCV virus, as assessed by real-time PCR. ZnO-NPs at doses of 20, 40, 60, 80, and 100 g/mL inhibited MCV replication by 17.8, 27.3, 53.3, 62.5, and 75.9%, respectively, according to estimates based on the viral load
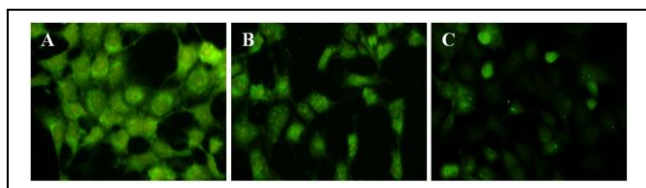
Figure 6. The immunofluorescence approach was used to examine the effect of ZnO-NPs on the expression of MCV antigens in Vero cells. In **A)**, the viral control was used; in **B)**, the cell control was used; and in **C)**, MCV-infected cells were treated with 100 g/mL Al₂O₃-NPs. The degree of fluorescence signals in HSV-1 infected cells treated with ZnO-NPs was shown to significantly diminish virus control, indicating that ZnO-NPs may have a potential antiviral impact on the expression of MCV. **C)**, the green spots represent viral antigens expressed in the various cell compartments, which were detected using a fluorescein isothiocyanate and goat anti-human IgG staining

4. Discussion

In the United States, no FDA-approved antiviral medication is available to treat MCV, a widespread viral skin infection that affects adults and children alike. Because of the difficulty of proliferating this poxvirus in cell culture, several efforts to develop chemicals that may limit MCV infection have been thwarted. Antiviral medications, such as acyclovir, have shown antiviral effectiveness in vitro against herpes virus and cytomegalovirus. Guan, Nuth (9) on the other hand, discovered that acyclovir had no inhibitory impact on the mD4 gene of MCV. Discovering novel and efficient anti-influenza medicines is thus an urgent need. When compared to traditional medical procedures, the use of nanoparticles offers several benefits. Effectiveness at lower doses, Strong antivirals against drug-resistant viruses, and Low-cost production are also essential considerations in therapy (24, 25). In the present work, we employed the MCV virus as a model and evaluated the antiviral activities of ZnO-NPs on the MC virus using this model. A series of in vitro cell culture studies were carried out to accomplish this goal, and the results were published in Science. Our findings indicate that ZnO-NPs have a higher antiviral impact and lower cytotoxicity, which is critical in improving antiviral activity against the MC virus and decreasing cell

cytotoxicity in Vero cells, respectively. As a consequence of our latest study, we discovered that ZnO-NP was related to increased antiviral efficacy against HSV-2 virions and decreased cytotoxicity in human vaginal epithelium and HeLa cells (24). In accordance with these findings, Duggal, Jaishankar (26) Performed ZnO-NPs have the ability to inhibit herpes simplex virus infection of cultured corneas. Design, Synthesis and evaluation of nano-systems for biomedical applications It has opened broad horizons for researchers to treat various diseases, including cancer, microbial diseases, and especially viral diseases (27-31). Gilles and Laure mentioned that MCV might be treated by ZnO cream containing colloidal oatmeal cream extracts (32). The same study reported inhibition of the H1N1 virus by ZnO-NPs (33). Other studies recorded the effects of ZnO-NPs on herpes simplex type-1 viruses and skin viruses that caused warts in humans (34, 35). The mechanisms responsible for the antibacterial and antiviral effects of ZnO-nanoparticles involved the formation of H_2O_2 from the ZnO-NPs surface, representing one of the most effective methods for decreasing bacterial growth. The inhibition capability of H_2O_2 occurs because the living cells produce catalase, which transfers hydrogen peroxidase to oxygen and H_2O.

(O) atoms attract electrons from the wall of viruses or bacteria (negative charge), furthermore destruction of the structure of the protein and the structure of the lipid of the cell surface. The cells become damaged after the oxidization process, wholly or partially (36). Ibanez, Farias (37) found that ZnO-NP kills some tumour cells, enhancing in removing the problem related to chemotherapy drugs (because the anticancer drug cannot distinguish between normal and tumour cells). Finally, the FDA recognizes ZnO as a safe (GRAS) material (38) and could be used as a food additive. Some foods, such as cereals, nutrition bars, and drinks, contain that mineral at small levels to boost nutrition. Several reports used ZnO in nutrition products because the ZnO-NPs have antibacterial effects against pathogens, and also, ZnO-NPs can increase thermal and

mechanical resistance. ZnO-NPs are used in many applications, such as glass, polypropylene, low-density polyethene, chitosan, paper, and polyurethane and have shown benefits (38). The results revealed that ZNO-NPs could inhibit the viral multiplication by blocking the attachment and prevention of the bacteria entrance of the virus inside the cells and preventing the spreading virus among the cells.

In summary, according to our findings, we show for the first time that ZnO NPs are associated with significant antiviral potency against MCV. ZnO NPs have broad-spectrum anti-MCV activity, providing new pharmacological opportunities. The antiviral behaviour of ZNO-NPs is thought to be explained by various mechanisms, such as the production of ROS by free Zn ions from NPs, which may contribute to MCV inactivation through viral protein oxidation or viral genome destruction.

Authors' Contribution

S. A. -M, A. K. A, and H. A., Methodology: S. A. -M, A. K. A, Validation: S.A.-M, A. K. A, B. B, Formal Analysis: B. B, Investigation: S. A. -M, A. K. A., Resources: S. A. -M, A. K. A, H., B. B., Writing–Original Draft Preparation: S. A.-M, A. K. A., Writing – Review and Editing: S. A. -M., Supervision: S. A. -M, A. K. A.

Conflict of Interest

The authors declare that they have no conflict of interest.

References

1. Harvey IB, Wang X, Fremont DH. Molluscum contagiosum virus MC80 sabotages MHC-I antigen presentation by targeting tapasin for ER-associated degradation. PLoS Pathog. 2019;15(4):1007711.

2. Nandhini G, Rajkumar K, Kanth KS, Nataraj P, Ananthakrishnan P, Arunachalam M. Molluscum contagiosum in a 12-year-old child–report of a case and review of literature. J Int Oral Health. 2015;7(1):63.

3. Chen X, Anstey AV, Bugert JJ. Molluscum contagiosum virus infection. Lancet Infect Dis. 2013;13(10):877-88.

4. Forbat E, Al-Niaimi F, Ali FR. Molluscum Contagiosum: Review and Update on Management. Pediatr Dermatol. 2017;34(5):504-15.

5. Leung AKC, Barankin B, Hon KLE. Molluscum Contagiosum: An Update. Recent Pat Inflamm Allergy Drug Discov. 2017;11(1):22-31.

6. Shisler JL. Immune evasion strategies of molluscum contagiosum virus. Adv Virus Res. 2015;92:201-52.

7. Zorec TM, Kutnjak D, Hosnjak L, Kusar B, Trcko K, Kocjan BJ, et al. New Insights into the Evolutionary and Genomic Landscape of Molluscum Contagiosum Virus (MCV) based on Nine MCV1 and Six MCV2 Complete Genome Sequences. Viruses. 2018;10(11).

8. Meza-Romero R, Navarrete-Dechent C, Downey C. Molluscum contagiosum: an update and review of new perspectives in etiology, diagnosis, and treatment. Clin Cosmet Investig Dermatol. 2019;12:373-81.

9. Guan H, Nuth M, Zhukovskaya N, Saw YL, Bell E, Isaacs SN, et al. A novel target and approach for identifying antivirals against molluscum contagiosum virus. Antimicrob Agents Chemother. 2014;58(12):7383-9.

10. Debing Y, Neyts J, Delang L. The future of antivirals: broad-spectrum inhibitors. Curr Opin Infect Dis. 2015;28(6):596-602.

11. Albukhaty S, Al-Musawi S, Abdul Mahdi S, Sulaiman GM, Alwahibi MS, Dewir YH, et al. Investigation of Dextran-Coated Superparamagnetic Nanoparticles for Targeted Vinblastine Controlled Release, Delivery, Apoptosis Induction, and Gene Expression in Pancreatic Cancer Cells. Molecules. 2020;25(20).

12. Al-Musawi S, Hadi AJ, Hadi SJ, Hindi NKK. Preparation and characterization of folated chitosan-magnetic nanocarrier for 5-fluorouracil drug delivery and studying its effect in bladder cancer therapy. J Glob Pharm Technol. 2019;11:628-37.

13. Al-Musawi S, Kadhim MJ, Hindi NKK. Folated-nanocarrier for paclitaxel drug delivery in leukemia cancer therapy.J Pharm Sci Res. 2018;10(4):749-54.

14. Albukhaty S, Al-Bayati L, Al-Karagoly H, Al-Musawi S. Preparation and characterization of titanium

dioxide nanoparticles and in vitro investigation of their cytotoxicity and antibacterial activity against Staphylococcus aureus and Escherichia coli. Anim Biotechnol. 2022;33(5):864-70.

15. Al-Kaabi WJ, Albukhaty S, Al-Fartosy AJM, Al-Karagoly HK, Al-Musawi S, Sulaiman GM, et al. Development of Inula graveolens (L.) Plant Extract Electrospun/Polycaprolactone Nanofibers: A Novel Material for Biomedical Application. Appl Sci. 2021; 11(2).

16. Al-Kinani MA, Haider AJ, Al-Musawi S. Design and Synthesis of Nanoencapsulation with a New Formulation of Fe@Au-CS-CU-FA NPs by Pulsed Laser Ablation in Liquid (PLAL) Method in Breast Cancer Therapy: In Vitro and In Vivo. Plasmonics. 2021;16(4):1107-17.

17. Al-Musawi S, Albukhaty S, Al-Karagoly H, Sulaiman GM, Alwahibi MS, Dewir YH, et al. Antibacterial Activity of Honey/Chitosan Nanofibers Loaded with Capsaicin and Gold Nanoparticles for Wound Dressing. Molecules. 2020;25(20).

18. Al-Musawi S, Albukhaty S, Al-Karagoly H, Sulaiman GM, Jabir MS, Naderi-Manesh H. Dextran-coated superparamagnetic nanoparticles modified with folate for targeted drug delivery of camptothecin. Adv Nat Sci Nanosci Nanotechnol. 2020;11(4):045009.

19. Haider A, Al-Kinani M, Al-Musawi S. Preparation and Characterization of Gold Coated Super Paramagnetic Iron Nanoparticle Using Pulsed Laser Ablation in Liquid Method. Key Eng Mater. 2021;886:77–85.

20. Chakravarty M, Vora A. Nanotechnology-based antiviral therapeutics. Drug Deliv Transl Res. 2021;11(3):748-87.

21. Albukhaty S, Al-Karagoly H, Dragh MA. Synthesis of zinc oxide nanoparticles and evaluated its activity against bacterial isolates. J Biotech Res. 2020;11:47-53.

22. Lallo da Silva B, Abucafy MP, Berbel Manaia E, Oshiro Junior JA, Chiari-Andreo BG, Pietro RCR, et al. Relationship Between Structure And Antimicrobial Activity Of Zinc Oxide Nanoparticles: An Overview. Int J Nanomedicine. 2019;14:9395-410.

23. Sirelkhatim A, Mahmud S, Seeni A, Kaus NHM, Ann LC, Bakhori SKM, et al. Review on Zinc Oxide Nanoparticles: Antibacterial Activity and Toxicity Mechanism. Nanomicro Lett. 2015;7(3):219-42.

24. Antoine TE, Mishra YK, Trigilio J, Tiwari V, Adelung R, Shukla D. Prophylactic, therapeutic and neutralizing effects of zinc oxide tetrapod structures against

herpes simplex virus type-2 infection. Antiviral Res. 2012;96(3):363-75.

25. Milovanovic M, Arsenijevic A, Milovanovic J, Kanjevac T, Arsenijevic N. Chapter 14 - Nanoparticles in Antiviral Therapy. In: Grumezescu AM, editor. Antimicrobial Nanoarchitectonics: Elsevier; 2017. p. 383-410.

26. Duggal N, Jaishankar D, Yadavalli T, Hadigal S, Mishra YK, Adelung R, et al. Zinc oxide tetrapods inhibit herpes simplex virus infection of cultured corneas. Molecular vision. 2017;23:26.

27. Al-Kinani MA, Haider AJ, Al-Musawi S. High Uniformity Distribution of Fe@Au Preparation by a Micro-Emulsion Method. IOP Conference Series: Materials Science and Engineering. 2020;987(1):012013.

28. Al-Kinani MA, Haider AJ, Al-Musawi S. Design, Construction and Characterization of Intelligence Polymer Coated Core–Shell Nanocarrier for Curcumin Drug Encapsulation and Delivery in Lung Cancer Therapy Purposes. J Inorg Organomet Polym Mater. 2021;31(1):70-9.

29. Al-Musawi S, Albukhaty S, Al-Karagoly H, Almalki F. Design and Synthesis of Multi-Functional Superparamagnetic Core-Gold Shell Coated with Chitosan and Folate Nanoparticles for Targeted Antitumor Therapy. Nanomaterials (Basel). 2020;11(1).

30. Al-Musawi S, Ibraheem S, Abdul Mahdi S, Albukhaty S, Haider AJ, Kadhim AA, et al. Smart nanoformulation based on polymeric magnetic nanoparticles and vincristine drug: a novel therapy for apoptotic gene expression in tumors. J Life. 2021;11(1):71.

31. Mohammed JA-A, Asim AB, Sharafaldin A-M, Mohammed JA, Ahmed K, Muntadher A. Investigation of Anti-MRSA and Anticancer Activity of Eco-Friendly Synthesized Silver Nanoparticles from Palm Dates Extract. Nano Biomed Eng. 2019;10(2): 157-69.

32. Mukherjee A, Mohammed Sadiq I, Prathna TC, Chandrasekaran N. Antimicrobial activity of aluminium oxide nanoparticles for potential clinical applications. Sci against Microb Pathog Commun Curr Res Technol Adv. 2011;1:245-51.

33. Maruzuru Y, Shindo K, Liu Z, Oyama M, Kozuka-Hata H, Arii J, et al. Role of herpes simplex virus 1 immediate early protein ICP22 in viral nuclear egress. J Virol. 2014;88(13):7445-54.

34. Dziuba N, Ferguson MR, O'Brien WA, Sanchez A, Prussia AJ, McDonald NJ, et al. Identification of cellular proteins required for replication of human

immunodeficiency virus type 1. AIDS Res Hum Retroviruses. 2012;28(10):1329-39.

35.   Zhang Q, Wang H, Ge C, Duncan J, He K, Adeosun SO, et al. Alumina at 50 and 13 nm nanoparticle sizes have potential genotoxicity. J Appl Toxicol. 2017;37(9):1053-64.

36.   Huet A, Huffman JB, Conway JF, Homa FL. Role of the Herpes Simplex Virus CVSC Proteins at the Capsid Portal Vertex. J Virol. 2020;94(24).

37.   Ibanez FJ, Farias MA, Gonzalez-Troncoso MP, Corrales N, Duarte LF, Retamal-Diaz A, et al. Experimental Dissection of the Lytic Replication Cycles of Herpes Simplex Viruses in vitro. Front Microbiol. 2018;9:2406.

38.   Carmody CM, Goddard JM, Nugen SR. Bacteriophage Capsid Modification by Genetic and Chemical Methods. Bioconjug Chem. 2021;32(3):466-81.